

METHODS ARTICLE

Fabrication, Rheological, and Compositional Characterization of Thermoresponsive Hydrogel from Cornea

Ghasem Yazdanpanah, MD, MPH, PhD,^{1,2,†} Yizhou Jiang, PhD,³ Behnam Rabiee, MD, MPH,¹ Meisam Omid, PhD,⁴ Mark I. Rosenblatt, MD, PhD, MBA,¹ Tolou Shokuhfar, PhD,² Yayue Pan, PhD,³ Alexandra Naba, PhD,⁵ and Ali R. Djalilian, MD¹

Fabricating thermoresponsive hydrogels from decellularized tissues is a trending and promising approach to develop novel biomaterials for tissue engineering and therapeutic purposes. There are differences in the characteristics of the produced hydrogels related to the source tissue as well as the decellularization and solubilization protocols used. Detailed characterization of the hydrogels will support the efforts to optimize their application as biomaterials for tissue engineering and therapeutics. Here, we describe an optimized method for fabricating an *in situ* thermoresponsive hydrogel from decellularized porcine cornea extracellular matrix (COMatrix), and provide a detailed characterization of its structure, thermoresponsive rheological behavior (heat-induced sol-gel transition), as well as exploring its protein composition using proteomics. COMatrix forms a transparent gel (10-min time to gelation) after *in situ* curing with heat, characterized by alteration in light absorbance and rheological indexes. The rheological characterization of heat-formed COMatrix gel shows similar behavior to common biomaterials utilized in tissue engineering. The fibrillar structure of COMatrix gel was observed by scanning electron microscopy showing that the density of fibers attenuates in lower concentrations. Mass spectrometry-based proteomic analysis revealed that COMatrix hydrogel is rich in proteins with known regenerative properties such as lumican, keratocan, and laminins in addition to structural collagen proteins (Data is available via ProteomeXchange with identifier PXD020606). COMatrix hydrogel is a naturally driven biomaterial with favorable biomechanical properties and protein content with potential application as a therapeutic biomaterial in ocular regeneration and tissue engineering.

Keywords: porcine cornea, extracellular matrix, hydrogel, thermal sol-gel transition, rheology, matrisome proteomics

Impact Statement

Fabrication and application of decellularized porcine corneal extracellular matrix is an emerging approach for corneal tissue engineering and regeneration. There are several protocols for decellularization of porcine cornea with various efficiencies. Here, we are presenting an optimized protocol for decellularization of porcine cornea followed by fabrication of a thermoresponsive hydrogel from the decellularized cornea matrix. Moreover, the fabricated hydrogel was rheologically and compositionally characterized as crucial features to be employed for further application of this hydrogel in corneal tissue engineering and regeneration.

Introduction

CORNEAL INJURIES AND diseases are a major cause of blindness worldwide. At present, the most effective therapy for corneal blindness is corneal transplantation,

which is only available to <5% of new cases worldwide.¹ Donor organ shortage, expensive and skill-based surgical procedures and graft are major challenges of corneal transplantation.^{2,3} Therefore, tissue engineering approaches have been used to overcome this obstacle. Many

¹Department of Ophthalmology and Visual Sciences, Illinois Eye and Ear Infirmary, University of Illinois at Chicago, Chicago, Illinois, USA.

Departments of ²Bioengineering and ³Mechanical and Industrial Engineering, University of Illinois at Chicago, Chicago, Illinois, USA.

⁴School of Dentistry, Marquette University, Milwaukee, Wisconsin, USA.

⁵Department of Physiology and Biophysics, University of Illinois at Chicago, Chicago, Illinois, USA.

[†]ORCID ID (<https://orcid.org/0000-0002-7518-8701>).

natural or synthetic biomaterials have been investigated as potential candidates for corneal regeneration to mimic the unique characteristics of corneal tissue such as transparency and distinctive biomechanical properties. Most of these studies have utilized natural biomaterials such as combinations of collagens, gelatin, and alginate.^{4–6}

The foremost drawback of these materials is that they are not representative of the corneal tissue composition and their sources are often from other organs, such as the skin and tendon.^{6–9} Thus, to fabricate a biomaterial/scaffold as a representative of naive corneal tissue with balanced composition of collagens, glycoproteins, and sulfated glycosaminoglycans,^{10,11} two approaches have been developed to mimic natural corneal microenvironment. First, decellularization of corneas followed by recellularization¹²; second, fabricating hydrogels from decellularized corneal extracellular matrix (ECM) with ability of self-assembly at body temperature (37°C).^{10,11,13–16} The advantage of the latter over the former approach for ocular regenerative medicine is that a self-assembled hydrogel could be applied *in situ* for regeneration of the corneal stroma or as an ocular surface bandage.

Recent studies on the biomaterials fabricated from other decellularized tissues have shown that these biomaterials can not only be applied as tissue engineering scaffolds, but also have healing effects that have not been observed in more purified natural biomaterials like collagens and gelatin.^{11,17,18} Moreover, corneal ECM-derived hydrogels provide a proper microenvironment for incorporating stem cells, which results in enhancing their differentiation and regenerative effects.¹⁴

Fabricating and utilizing thermoresponsive hydrogels from ocular tissues for further therapeutic and tissue engineering applications is a rapidly emerging field in ophthalmic regenerative medicine. A few studies have reported the production of thermoresponsive hydrogels from decellularized porcine or bovine corneas.^{10,11,13,14} However, as of today, there is no detailed, comprehensive, and optimized fabrication process. Studies have also examined the composition of the ECM of the cornea.¹⁹ Yet, we lack a detailed compositional, structural, and rheological characterization of the produced hydrogels from corneas.

Here, we present an optimized protocol decellularize and then digest porcine corneas to produce a thermoresponsive COrneal extracellular Matrix (COMatrix) hydrogel. We further provide the first detailed characterization of the protein composition of COMatrix hydrogel by mass spectrometry-based proteomics and have compared it with the ECM of human amnion, a material commonly used clinically in ophthalmic care. Furthermore, detailed structural, thermal gelation kinetics, and rheological properties of fabricated corneal ECM hydrogel are presented. Furthermore, the detailed and comprehensive methodological protocols for porcine cornea decellularization and fabrication of thermoresponsive hydrogel from the decellularized tissue could pave the way for researchers to produce this natural biomaterial. The methods and results of this study could be used as a reference for future studies to develop novel approaches for corneal tissue engineering and regeneration.

Method

Fabrication of COMatrix hydrogel

The fabrication of COMatrix hydrogel including decellularization and solubilization in addition to performed characterization analyses are given in Figure 1. Fresh intact porcine eyeballs were obtained from a certified abattoir (Park Packing Co., Inc., Chicago, IL). Under sterile conditions, the porcine corneas (PCs) were dissected and washed with phosphate-buffered saline (PBS, 1×) containing 1% gentamicin, 1% penicillin, and 1% streptomycin. Human amnion, an ECM-rich tissue in clinical use, was used as a positive control. To obtain human amnion, placentas were obtained from elective caesarean sections following mother's written informed consent, under an approved protocol by the University of Illinois at Chicago Institutional Review Board here is the part mentioning the IRB approval for harvesting human placentas.

The placentas were transferred to the lab immediately and human amnions were peeled and dissected in sterile condition as described earlier.²⁰ The amnions were washed with PBS (1×) containing 1% gentamicin, 1% penicillin, and 1% streptomycin.

The decellularization process for PCs and human amnions were performed as described before¹¹ with some optimization to improve efficiency (Illustrated in Fig. 1). The PCs were cut into pieces with an average size of 2×2 mm² and amnions were cut into 1×1 cm² pieces. The tissue pieces were first stirred in 20 mM ammonium hydroxide solution (Sigma) containing 0.5% Triton X-100 (Fisher Scientific) in distilled water for (pH 10) 4 h for decellularization. Tissues were then transferred to 10 mM Tris-HCl (Sigma) containing 0.5% EDTA (Fisher Scientific) in distilled water (pH 7.5) and stirred for 24 h at room temperature. After that, PCs and amnion pieces stirred in 10 mM Tris-HCl containing 1% (v/v) Triton X-100 (pH 7.5) for 24 h at 37°C. To remove the DNA remnants, the tissue fragments were agitated in 50 mM Tris-HCl containing 7.5 U/mL deoxyribonuclease (Sigma) in molecular biology grade water (pH 7.5; Fisher Scientific) for 16 h at 37°C. To further remove cell remnants and chemicals, the samples were stirred in PBS (pH 7.5) for 48 h while changing the PBS twice per day. The bioburden of decellularized PCs and amnion pieces was reduced by stirring in 0.1% peracetic acid (32 wt% in dilute acetic acid; Sigma) in 4% ethanol in molecular biology grade water for 20 h. After stirring the tissues in molecular biology grade water three times for 2 h, the tissues were snap frozen in liquid nitrogen and lyophilized for 48 h at –55°C and <0.133 mBar. The lyophilized tissues were then stored at –80°C until further experiments for no more than 6 months.

To fabricate COMatrix hydrogel from decellularized PC-ECM (illustrated in Fig. 1), lyophilized tissue pieces were cryomilled using a freezer mill (Spex 6700). The resultant fine powder was sieved using a mesh (size 40; Sigma) and partially digested by slow stirring in 0.01 M HCl (20 mg/mL) containing 1 mg/mL pepsin (>400 U/mg; Sigma) for 72 h at room temperature. To form a hydrogel, the digested PC-ECM was neutralized to pH 7 using one-ninth 0.1 M NaOH and one-tenth PBS 10×, while on the ice. The hydrogel was diluted to the desired concentrations using PBS. To induce gelation, the cool COMatrix hydrogel was incubated at 37°C for 30–45 min. Decellularized human amnions were solubilized using the same protocol for the PCs.

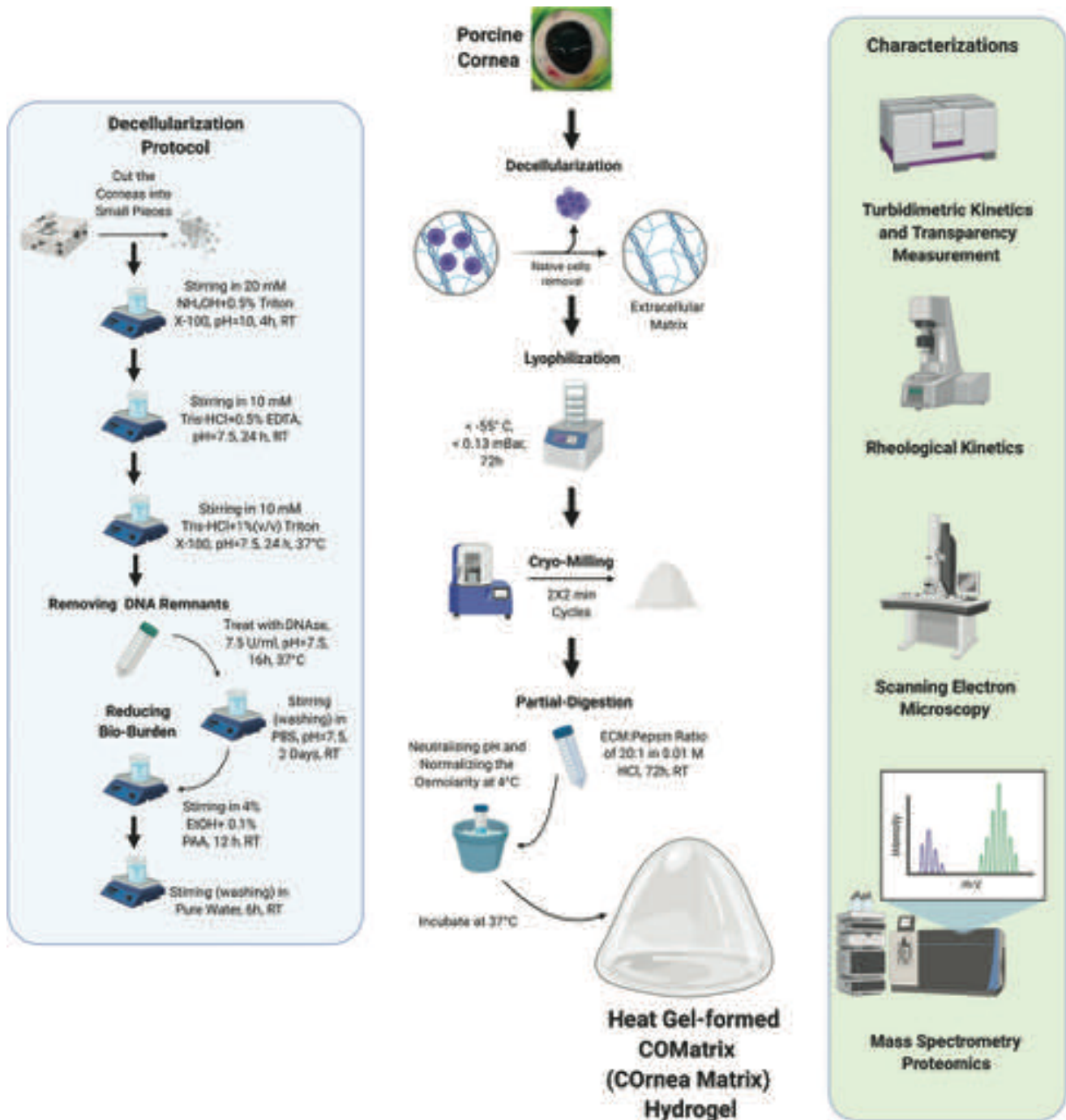


FIG. 1. Illustration of optimized protocol for decellularization of porcine cornea (left) fabrication of thermoresponsive cornea matrix (COMatrix) hydrogel (middle), and the performed characterizations in this study (right). Color images are available online.

Experiment

Evaluating the efficiency of decellularization

The efficiency of decellularization was assessed by hematoxylin and eosin (H&E) and DAPI staining. The decellularized tissue pieces were fixed in the Tissue-Tek[®] optimum cutting temperature solution and froze on dry ice. After sectioning using Cryostat (Fisher Scientific) and transferring on the histological slides, the sections were fixed in 4% paraformaldehyde for 15 min and washed with

deionized (DI) water. The slides incubated in hematoxylin (Fisher Scientific) for 2 min followed by washing with DI water. After that, the slides were briefly treated with 70% ethanol/1% HCl and washed with DI water. The slides were then stained with eosin (Fisher Scientific) for 7 min and then washed briefly with 95% ethanol. The sections were then dehydrated with 100% ethanol for 10 min followed by incubating in xylene (Fisher Scientific) for 10 min. After drying in room temperature, one drop of mountant with DAPI (ProLong[™] Diamond Antifade Mountant with DAPI)

was applied on the slide and a coverslip (22×40 mm) was placed on the tissue sections and sealed with nail polish solution. The stained tissue sections were visualized and imaged with a fluorescence/light microscope (Zeiss).

Compositional characterization of COMatrix hydrogel

Biochemical contents of COMatrix hydrogel. Relevant assays to measure amount of DNA, total collagen, and sulfated glycosaminoglycans (sGAGs) in COMatrix hydrogel and solubilized amnion (both pepsin digested decellularized ECMs) were performed. Beforehand, the samples were digested in papain extraction solution [1:1 v/v, 50 mL of 0.2 sodium phosphate buffer (pH 6.4), 400 mg sodium acetate, 200 mg EDTA, 40 mg cysteine HCl, 250 μ L of papain suspension (Sigma; p3125) containing 5 mg of enzyme) overnight at 65°C. The DNA contents of samples were quantified by purifying the genomic double-stranded DNA using a commercially available kit (Catalog #G1N70; Sigma) per the manufacturer's protocol. The concentration of the DNA samples obtained was further measured using a NanoDrop Microvolume Spectrophotometer (Fisher Scientific) at 260 nm. Total collagen content was measured using the hydroxyproline assay.²¹ In brief, 100 μ L of papain-digested COMatrix hydrogel and solubilized amnion were added to 100 μ L of 4 N NaOH separately and hydrolyzed by autoclaving for 15 min. After cooling the samples to room temperature, 100 μ L of 4 N HCl was added. Then, 100 μ L of the resultant solution was mixed with 100 μ L of chloramine-T solution and incubated for 20 min at room temperature. After that, 200 μ L of p-dimethylaminobenzaldehyde (p-DAB) solution was added to the mixture and the tubes were incubated at 60°C for 30 min, followed by immediate soaking of the tubes in room temperature water for 5 min to quench the reaction. A 100 μ L sample of the prepared mixture was transferred to a 96-well plate in triplicate, and the mixture absorbance was measured at 540 nm. Hydroxyproline dissolved in sodium-phosphate buffer with concentrations of 200, 100, 50, 25, 12.5, 6.25, 3.125, 1.56, and 0 mg/mL was used to draw the standard curve.

The sGAG content was measured using 1,9-dimethyl methylene blue (DMMB) assay. DMMB working solution was the combination of 5 mL of formate solution (0.25 g sodium formate in 24 mL of 1 M guanidine hydrochloride (GuHCl) and 0.2975 mL of >95% formic acid), 12.5 mL 200 proof anhydrous ethanol, 6.4 mg of DMMB (Sigma), and 7.5 mL ultrapure water. One milliliter of DMMB working solution was added to 100 μ L of papain-digested ECM or standard, agitated at 150 rpm for 30 min in room temperature, and centrifuged to precipitate a sGAG-dye complex. The supernatant was aspirated, and 1 mL decomplexation solution was added to the pellet, before being agitated at 150 rpm for 30 min at room temperature. The samples were transferred to a 96-well plate in triplicate, and absorbance was measured at 650 nm. Serial dilution of chondroitin sulfate (Sigma) from 200 μ g/100 μ L to 0 μ g/100 μ L was used as standards.

Proteomic analysis

To evaluate the quality of fabricated decellularized corneal ECMs digested with pepsin, the COMatrix hydrogel (two replicates) and pepsin-solubilized amnion

(two replicates) were compared with rat tail collagen and pepsin-digested bovine tendon collagen using sodium dodecyl sulfate–polyacrylamide gel electrophoresis (SDS-PAGE). About 7.5 μ L of each sample (6 mg/mL) was mixed with 3.75 μ L LDS 4× sample buffer, 1.5 μ L 10× reducing agent (dithiothreitol), and 2.25 μ L DI H₂O (all are NuPAGE; Fisher Scientific) to a total volume of 15 μ L. After vortexing and spinning down, the tubes were heated at 95°C in a heating block for 15 min. Then, the samples were loaded into a 4–12% Bis-Tris gel (10 wells, 12 μ L per well, NuPAGE; Fisher Scientific) and subjected to electrophoresis using SDS running buffer (NuPAGE; Fisher Scientific) and constant voltage (150 V) until the dye reached the bottom of the gel (~1.5 h). Afterward, the gel was washed with deionized water (3×5 min) and stained with Bio-Safe Coomassie Brilliant Blue G-250 (50 mL per gel; BIO-RAD) for 1 h with gentle agitation. The stained gel was then rinsed with deionized water for 30 min to visualize distinct bands.

To explore the composition of fabricated COMatrix hydrogel proteomic analyses were performed using an established mass spectrometry (LC-MS/MS) protocol for evaluating the “matrisome.”^{22,23} One COMatrix hydrogel sample and one human amnion were compositionally characterized. To digest the samples into peptides for mass spectrometric analyses, a previously published method was used with minor modifications.²³ The samples were dehydrated in a low attachment tube using vacuum concentrator to retrieve 5 mg of sample. The samples were then re-suspended in 8 M urea (200 μ L) plus 4 μ L of 500 mM dithiothreitol (final concentration 10 mM) followed by agitation at 1500 rpm for 2 h at 37°C for denaturation/reduction. After that, to alkylate proteins 10 μ L of 500 mM iodoacetamide (diluted in HPLC-grade water) was added to reach the final concentration of 25 mM and incubated for 30 min at room temperature in the dark. Deglycosylation of proteins was performed by diluting to 2 M urea by adding 642 μ L of 100 mM ammonium bicarbonate pH 8.0 and then adding 2 μ L of PNGaseF (500 U/ μ L) followed by agitation at 1500 rpm for 2 h at 37°C. The digestion of proteins into peptides was achieved by adding mass spectrometry-grade endoproteinase LysC (final amount of 1 μ g) and agitating at 1500 rpm for 2 h at 37°C followed by adding trypsin (final amount of 3 μ g) and shaking at 1400 rpm at 37°C overnight. The second digestion was performed by adding a second aliquot of trypsin (final amount of 1.5 μ g) and shaking for an additional 2 h at 1500 rpm and 37°C. To inactivate the trypsin, the samples were acidified by freshly prepared 50% trifluoroacetic acid (TFA) in HPLC-grade water to pH <2, and then centrifuged at 16,000 g for 5 min at room temperature. The supernatant was transferred to a clean low-attachment tube and desalted using a desalting spin column (Pierce™ Peptide Desalting Spin Columns; Fisher Scientific) per the manufacturer's instructions. After desalting, the samples were dried in a speed-vac system and reconstituted in a freshly prepared 5% acetonitrile and 0.1% formic acid in HPLC-grade water. The peptide concentration was measured by spectrophotometry (280 nm) and analyzed by mass spectrometry (LC-MS/MS).

To perform LC-MS/MS, samples (400 ng per run) were run on Thermo Fisher Orbitrap Velos Pro coupled with Agilent NanoLC system (Agilent, Santa Clara, CA). The LC columns (15 cm×75 μ m ID, Zorbax 300SB-C18) were

purchased from Agilent. Two technical replicates were acquired for each sample. Samples were analyzed with a 120-min linear gradient (0–35% acetonitrile with 0.1% formic acid) and data were acquired in a data-dependent manner, in which MS/MS fragmentation is performed on top 12 intense peaks of every full MS scan. Full MS scans were acquired in the Orbitrap mass analyzer over m/z 400–2000 range with resolution 30,000 (m/z 400). The target value was $1.00E+06$. The 12 most intense peaks with charge state ≥ 2 were fragmented in HCD collision cell with normalized collision energy of 30% and excluded for 30 s after 2 counts within a mass window of 10 ppm. Tandem mass spectrum was acquired in the Orbitrap mass analyzer with resolution of 7500. The target value was $5.00E+04$. The ion selection threshold was 5000 counts, and the maximum allowed ion accumulation times were 500 ms for full scans and 250 ms for HCD. RAW files were converted into .mgf files using MSConvert (from ProteoWizard). All MS/MS samples were analyzed using Mascot (Matrix Science, London, United Kingdom; version 2.6.2).

Porcine cornea samples: database search and protein identification criteria. Mascot was set up to search the Uniprot_pig_all_20201006 database (49,792 entries) assuming the digestion enzyme stricttrypsin. Mascot was searched with a fragment ion mass tolerance of 0.30 Da and a parent ion tolerance of 15 ppm. O-110 of pyrrolysine, $u+49$ of selenocysteine, and carbamidomethyl of cysteine were specified in Mascot as fixed modifications. Gln→pyro-Glu of the n-terminus, deamidated of asparagine and glutamine and oxidation of lysine, methionine, and proline were specified in Mascot as variable modifications. Scaffold (version Scaffold_4.11.1; Proteome Software, Inc., Portland, OR) was used to validate MS/MS-based peptide and protein identifications. Peptide identifications (strict) were accepted if they could be established at $>98.0\%$ probability to achieve an FDR $<1.0\%$ by the Scaffold Local FDR algorithm. Protein identifications were accepted if they could be established at $>95.0\%$ probability and contained at least 1 identified peptide. Protein probabilities were assigned by the Protein Prophet algorithm²⁴ (Supplementary Table S1A).

Human amnion samples: database search and protein identification criteria. Mascot was set up to search the Uniprot-human_20201006 database (20,385 entries) assuming the digestion enzyme stricttrypsin. Mascot was searched with a fragment ion mass tolerance of 0.30 Da and a parent ion tolerance of 15 ppm. O-110 of pyrrolysine, $u+49$ of selenocysteine, and carbamidomethyl of cysteine were specified in Mascot as fixed modifications. Gln→pyro-Glu of the n-terminus, deamidated of asparagine and glutamine and oxidation of lysine, methionine, and proline were specified in Mascot as variable modifications. Scaffold was used to validate MS/MS-based peptide and protein identifications. Peptide identifications (strict) were accepted if they could be established at $>96.0\%$ probability to achieve an FDR $<1.0\%$ by the Scaffold Local FDR algorithm. Protein identifications were accepted if they could be established at $>96.0\%$ probability and contained at least 1 identified peptide (Supplementary Table S1B).

For both datasets, proteins that contained similar peptides and could not be differentiated based on MS/MS analysis

alone were grouped to satisfy the principles of parsimony. Proteins sharing significant peptide evidence were grouped into clusters. Mass spectrometry output was further annotated to identify ECM and non-ECM components using the matrisome list we have previously devised.^{25,26} In brief, matrisome components are classified as core-matrisome or matrisome-associated components, and further categorized into groups based on structural or functional features: ECM glycoproteins, collagens, or proteoglycans for core matrisome components; and ECM-affiliated proteins, ECM regulators, or secreted factors for matrisome-associated components.²⁵ To define the matrisome of the two sample type profiled: COMatrix and human amnion, we included proteins detected with at least two peptides in any of the two technical replicates, and for proteins detected with only one peptide, mandated they be detected in both technical replicates. The raw mass spectrometry have been deposited to the ProteomeXchange Consortium²⁷ using the PRIDE²⁸ partner repository with the dataset identifier PXD020606 and 10.6019/PXD020606.

Transparency and ultrastructural characterization of COMatrix hydrogel

To measure the transparency, 100 μ L of 4°C COMatrix hydrogel (5, 15, and 25 mg/mL, each triplicate) was loaded into a 96-well plate (~ 300 μ m thickness) and sol-gel transition was induced and completed by incubating at 37°C for 30 min. The light transmission of each well was then measured from 300 to 800 nm in a prewarmed plate reader to 37°C (BioTek™ Synergy™ H1 Hybrid).

The ultrastructure of heat-formed COMatrix hydrogel was observed using scanning electron microscopy (SEM). The samples (5, 10, and 15 mg/mL) were fixed with cold glutaraldehyde overnight and then dehydrated with serial dilutions of ethanol/hexamethyldisilazane (2:1, 1:1, 1:2, and 0:1, respectively, each step 30 min and allowed to evaporate in the last step). After that, the samples were sputter coated and visualized using a scanning electron microscope (JEOL JSM-IT500HR FESEM).

Gelation kinetics and rheological characterizations of COMatrix hydrogel

The sol-gel transition of thermoresponsive COMatrix hydrogel heated to 37°C was characterized by both turbidimetric assay and rheologic analysis. In turbidimetric assay, 50 μ L of cool COMatrix hydrogel (5, 15, and 25 mg/mL, each triplicate) was loaded in each well of a cold 96-well plate. Then, the absorbance of each well was measured every 2 min at 405 nm in a prewarmed (37°C) plate reader for 30 min.

To record the gelation course of COMatrix hydrogel with rheology, a rotational rheometer (Kinexus Ultra+; Malvern) with a parallel 25 mm plate and temperature controller was used. The rheometer bed was initially set to 12°C (assume that gelation is negligible in this temperature) and COMatrix hydrogel in different concentrations (15 and 25 mg/mL) was loaded. The parallel gap was set to 0.9 mm and mineral oil was applied and trimmed around the plate to prevent sample dryness during the experiment. The rheological indexes were measured with 0.159 Hz (1 rad/s) frequency and 0.5% strain. After 3 min of recording, the temperature was ramped

rapidly (in 25 s) to 37°C to induce gelation. The recording was continued for 50 min to characterize the gelation kinetics and measure the rheological shear moduli. Moreover, the rheological properties of heat formed hydrogel was evaluated by frequency and strain sweeps, in which shear elastic (G') and viscous (G'') moduli were recorded. In frequency sweep the frequency was changed from 0.1 to 10 Hz at 0.5% strain, and in strain sweep the average complex shear strain was changed from 0.1% to 100% at 0.159 Hz frequency. Three different samples were characterized for each concentration.

In vitro biocompatibility studies

To evaluate the biocompatibility of the fabricated COMatrix hydrogel, the viability and proliferation of human corneal epithelial cells (HCECs) and human corneal mesenchymal stem cells (hCMSCs) cultured *in vitro* with the hydrogel was evaluated. Immortalized HCECs were kindly provided by Dr. Deepak Shukla (Illinois Eye and Ear Infirmary, University of Illinois at Chicago).²⁹ HCECs were expanded in high-glucose DMEM (4500 mg/L; Fisher Scientific) containing 10% fetal bovine serum (Fisher Scientific) and 1× antibiotic–antimycotic (Fisher Scientific) for no more than 40 passages. HCECs were detached with TrypLE express enzyme (Fisher Scientific) for further culture on top of thermally formed COMatrix hydrogel. One hundred microliters of cold COMatrix hydrogel was pipetted in 96-well plate (~300 μm thickness) and incubated at 37°C for 45 min. Then, HCECs (2×10^3 cells/well) were cultured on top of the formed COMatrix hydrogel.

The hCMSCs were extracted from cadaveric human corneas as described before by our group.³⁰ The obtained hCMSCs were expanded in α -MEM (Fisher Scientific) containing 10% fetal bovine serum (Fisher Scientific) and 1× antibiotic–antimycotic (Fisher Scientific). HCECs at passage 3 were detached with TrypLE express enzyme (Fisher Scientific) for interactions with COMatrix hydrogel. One hundred microliters of cold COMatrix hydrogel was combined with 2×10^3 hCMSCs and transferred to a well of a 96-well plate and incubated in humidified incubator with 5% CO₂ at 37°C for 45 min. Then, the full media (150 μL) were added on top of the gel-formed hydrogel.

The viability of cultured cells with COMatrix hydrogel at days 1 and 16 was evaluated by staining with Calcein-AM (live cells), propidium iodide (PI; dead cells), and Hoechst 33342 (total cells, all from Sigma) for 1 h by incubating at 37°C in humidified atmosphere with 5% CO₂. The cells were imaged using ZEISS Cell Observer SD Spinning Disk Confocal Microscope (Zeiss), and the images were analyzed using ZEN Lite software (Zeiss). Also, to evaluate the proliferation of cells during *in vitro* culture with COMatrix hydrogel, a metabolic activity assay was performed using the Cell Counting Kit-8 (CCK-8; Sigma). Following the manufacturer's recommendation, 10 μL of the provided solution (WST-8) was added to each well containing 100 μL of complete media, after which the plate was incubated in humidified atmosphere with 5% CO₂ at 37°C for 2 h; and the optical density (OD) was measured at 450 nm representing the number of cells in each well. All experiments were conducted in triplicate.

Statistical analyses

Data are given as mean ± standard deviation (SD). Statistical analyses were performed by GraphPad Prism software version 8.3.0 (538) for Windows (GraphPad Software, San Diego, CA, www.graphpad.com) using *t*-test for comparing the means between two groups and one-way analysis of variance and Tukey posttest for more than two groups. Values of $p < 0.05$ were considered as statistically significant difference between groups.

Experimental Results

Compositional characterization of COMatrix hydrogel

The efficiency of decellularization and compositional profile of COMatrix was determined and compared with human amnion, a commonly used biological material for ophthalmic applications. PCs and human amnions underwent a series of treatments with hypotonic solutions containing nonionic detergents, chelating agents, and nuclease enzymes (Fig. 1). H&E and DAPI staining showed successful removal of the cells and nuclei, especially after treatment with DNase (Fig. 2A). Measuring the DNA remnant in decellularized tissues confirmed significant reduction after treatment with DNase ($p < 0.01$, Fig. 2B). The decellularization process did not significantly change the total collagen and sulfated glycosaminoglycans (sGAG) contents in both COMatrix and human amnion. The concentrations of total collagen in COMatrix and amnion after decellularization were 0.72 ± 0.1 mg and 0.71 ± 0.1 mg per mg, respectively ($p > 0.05$, Fig. 2C). The sGAG contents were 0.2 ± 0.03 mg and 0.12 ± 0.02 mg per mg, respectively ($p < 0.05$, Fig. 2D).

Proteomic characterization of COMatrix hydrogel composition

To evaluate the quality of fabricated ECM products from decellularized porcine cornea and human amnion, the samples were compared with commercial rat tail and bovine tendon collagens using SDS-PAGE. Figure 2E shows that COMatrix hydrogel and human amnion not only have similar protein contents to rat tail and bovine tendon collagens but also have additional proteins. Two different samples for COMatrix hydrogel and human amnion were loaded to show the reproducibility of the performed process.

The protein profiles of fabricated COMatrix hydrogel and solubilized human amnion were further evaluated using an established mass spectrometry protocol for analyzing the protein composition of ECMs, or the “matrisome,” of tissues.^{23,25} Computational annotation of mass spectrometry output classifies proteins into core, structural matrisome, and matrisome-associated proteins. The core-matrisome proteins are collagens, proteoglycans, and other ECM glycoproteins, and the matrisome-associated proteins are ECM regulators, ECM-affiliated proteins, and secreted factors.²⁵ The detected normalized peptide spectrum shows that >99% of both the COMatrix hydrogel and the decellularized human amnion are composed of ECM proteins (Fig. 3A) and more specifically of fibrillar type I collagen, encoded by the *Colla1* and *Colla2* genes. This result indicates efficient decellularization of both PCs and human amnion and maintaining the ECM and ECM-associated proteins in the

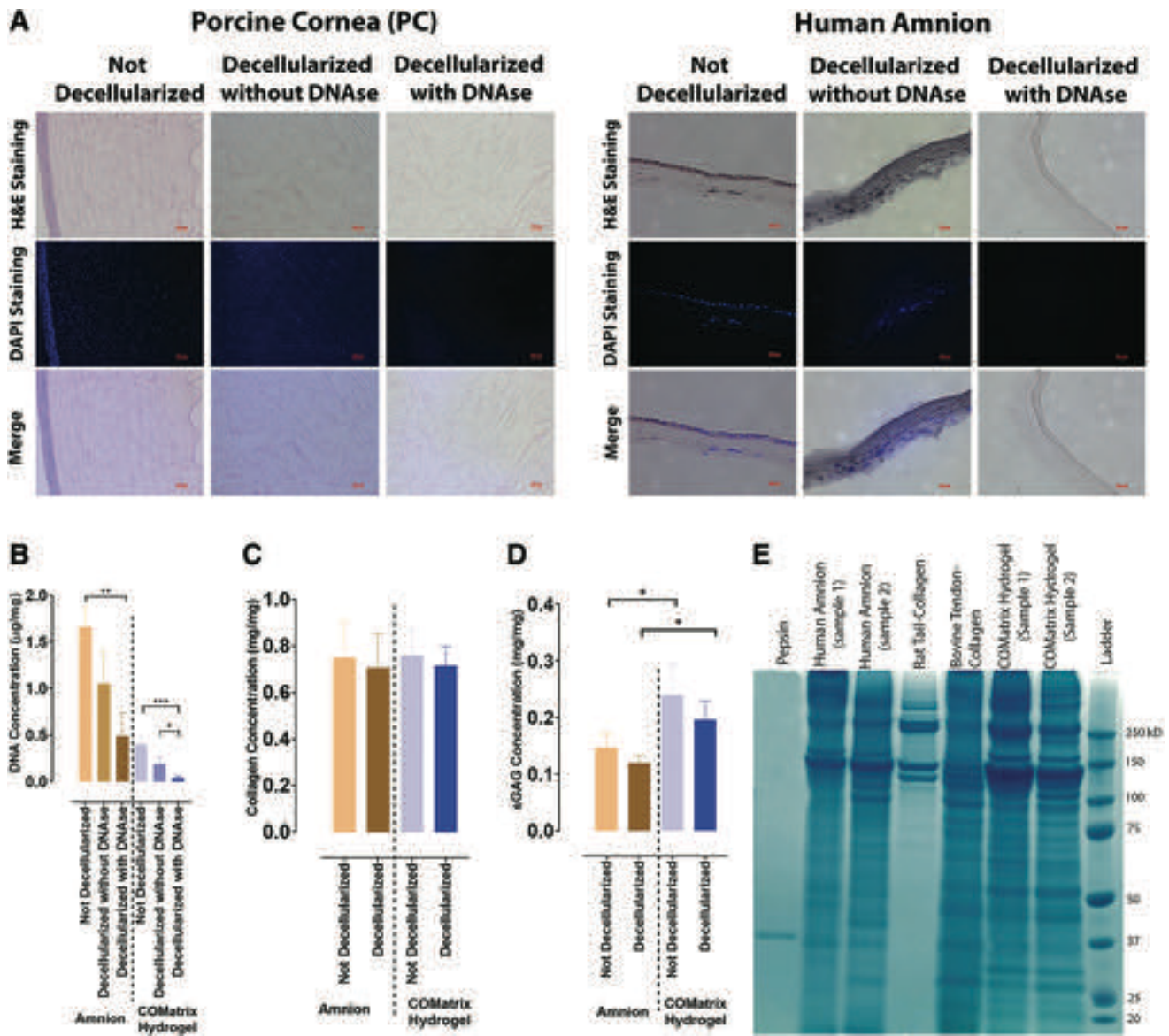


FIG. 2. (A) H&E staining of decellularized porcine cornea and human amnion indicating the role of DNase in removing genomic DNA. (B) DNA content of COMatrix hydrogel and pepsin-solubilized human amnion after decellularization with and without DNase. (C) Total collagen content of naive tissue and decellularized COMatrix hydrogel and pepsin-solubilized human amnion. (D) Total sGAG content of naive tissue and decellularized COMatrix hydrogel and pepsin-solubilized human amnion. (E) SDS-PAGE of COMatrix hydrogel and pepsin-solubilized human amnion in comparison with purified rat tail collagen and pepsin-digested bovine tendon collagen. *** $p < 0.001$; ** $p < 0.01$; * $p < 0.05$. sGAG, sulfated glycosaminoglycans; H&E, hematoxylin and eosin; SDS-PAGE, sodium dodecyl sulfate–polyacrylamide gel electrophoresis. Color images are available online.

samples. The analysis of technical replicates further confirms the reproducibility of our analytical pipeline (Supplementary Table S1A, B). The mass spectrometry results based on the matrisome subgroups are also presented in Figure 3B. With the criteria and strict thresholding applied, we detected 13 types of collagen (Supplementary Table S1A), 1 glycoprotein (the $\gamma 1$ chain of laminin), and 2 proteoglycans (lumican and keratocan) in the COMatrix hydrogel (Fig. 3B and Supplementary Table S1A), whereas we detected 15 collagens (Supplementary Table S1B), 3 ECM glycoproteins (periostin, the transforming growth factor beta-induced protein, and procollagen C-endopeptidase enhancer 1), 2 proteoglycans (lumican and

decorin), and 1 ECM-affiliated protein (annexin A2) in the solubilized human amnion constituted (Fig. 3B and Supplementary Table S1B). We also detected the proteoglycan fibromodulin, but with only 1 peptide in only 1 of the two COMatrix technical replicates (Supplementary Table S1A). The numbers of unique peptides and the total spectral counts in each sample run are summarized in Figure 3C and D, respectively. The Venn diagrams in Figure 3E and F indicate the number of identified matrisome proteins in each sample replicate. The low difference in detected matrisome proteins between the replicates in both COMatrix and human amnion samples indicates the high reproducibility of used proteomic approach.

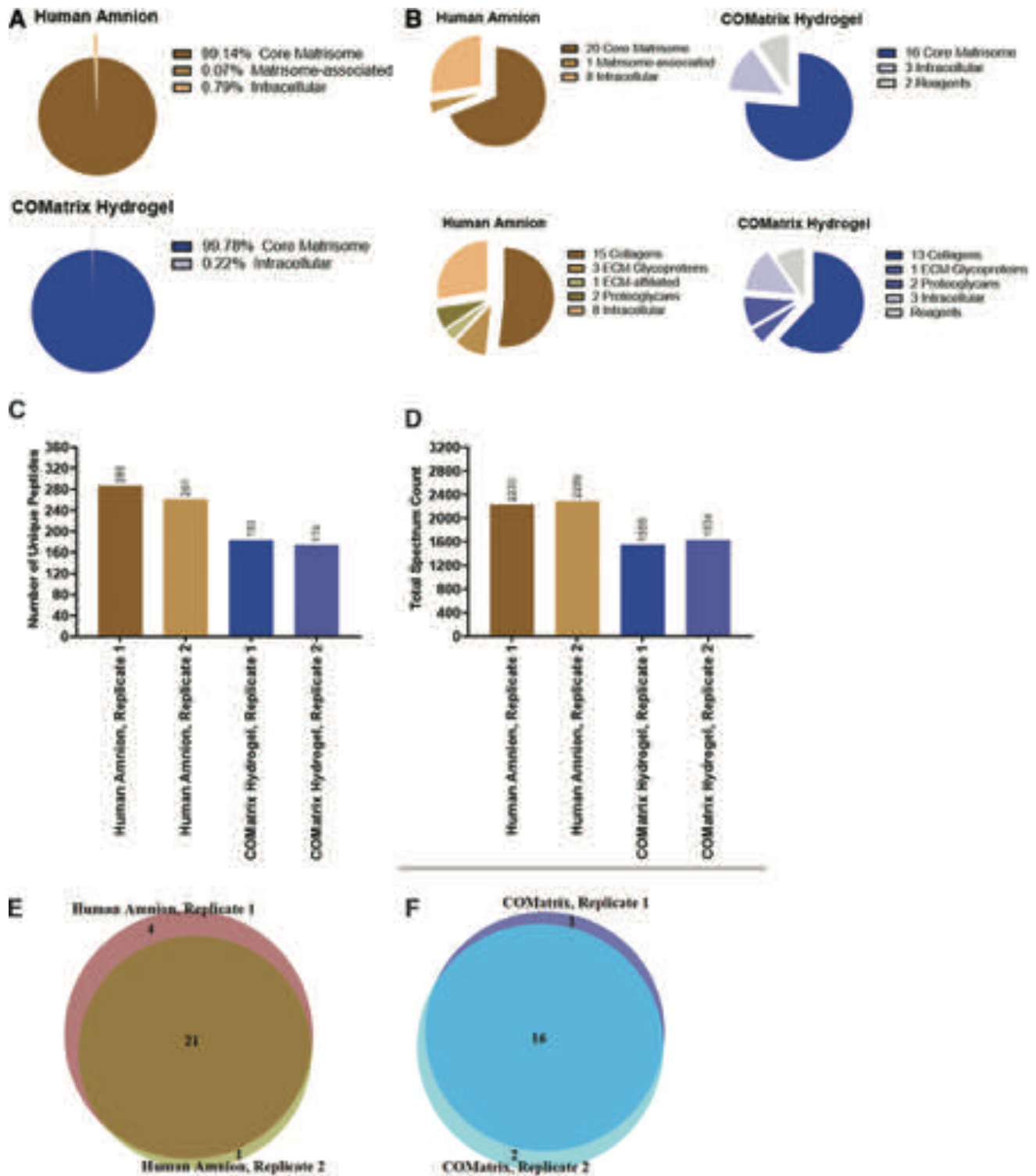


FIG. 3. The proteomic analyses of COMatrix hydrogel and pepsin-solubilized human amnion based on previously developed matrisome pipeline using LC-MS/MS.^{21,23} (A) Relative proportion of ECM and non-ECM proteins based on normalized spectral count. (B) Number of proteins in COMatrix hydrogel and pepsin-solubilized human amnion classified according to their matrisome categories (see Materials and Methods section). (C, D) Number of unique peptides and total spectral counts of identified proteins. (E, F) The number of detected proteins in each sample run of COMatrix hydrogel and human amnion. ECM, extracellular matrix. Color images are available online.

Figure 4 summarizes the protein overlap between COMatrix hydrogel and solubilized human amnion (Fig. 4A), as well as the identified matrisome proteins in all samples (Fig. 4B). We found that 10 matrisome proteins were common to both the COMatrix hydrogel and the ECM of

human amnion. Collagens were the most abundant proteins in both sample types as given in Figure 4B summarizing the normalized spectral counts for each matrisome protein in COMatrix hydrogel and solubilized human amnion samples, and which serves as a proxy to protein abundance. In summary, with this preliminary analysis, the protein composition of the COMatrix hydrogel is rich in proteins with known corneal regenerative effects, such as lumican, laminin, and keratocan.^{31–47} Lumican is the protein found in both COMatrix and human amnion digest.

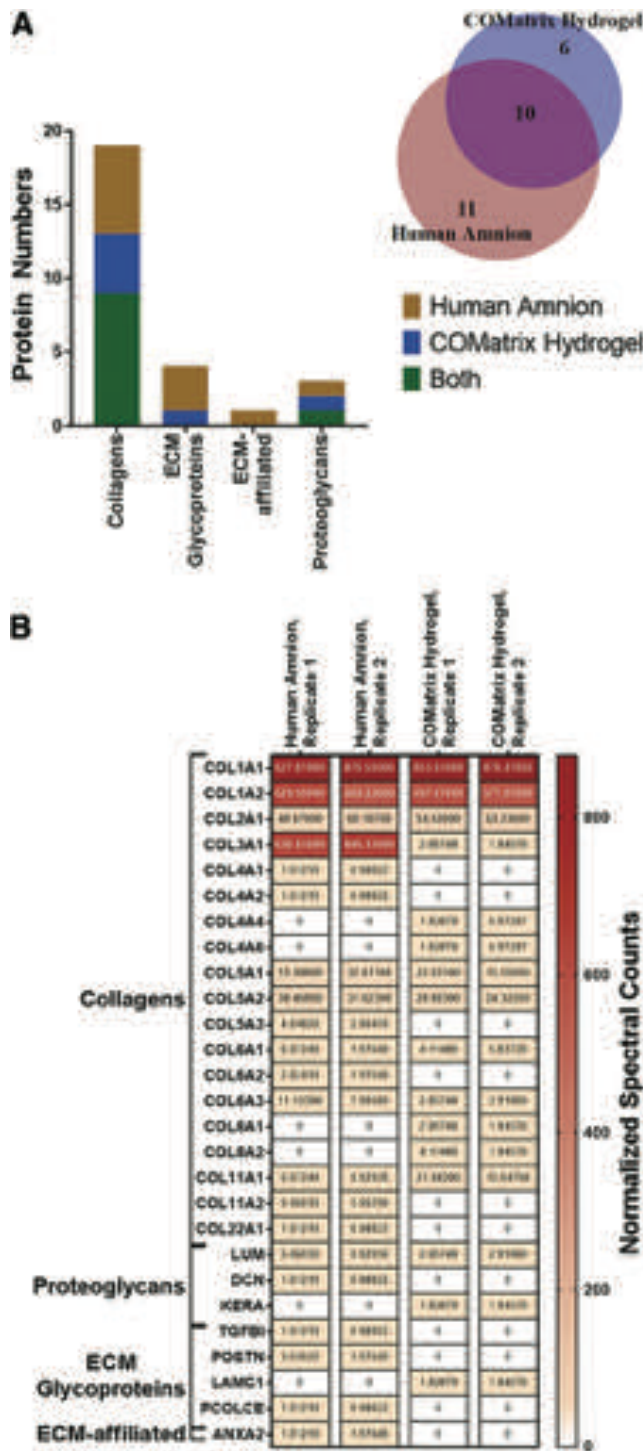


FIG. 4. (A) Summarizing the protein overlap between COMatrix hydrogel and solubilized human amnion. (B) The normalized spectral count of peptides for identified proteins in COMatrix hydrogel and solubilized human amnion samples (the detailed summary of detected proteins is available in Supplementary Table S1). Color images are available online.

Transparency and ultrastructure of COMatrix hydrogel

The heat-formed COMatrix gel is optically transparent as given in Figure 5A. Quantitative measurement of gel-formed COMatrix transparency shows high light transmission in visible spectrum (Fig. 5B). The light transmission of 15 mg/mL COMatrix hydrogel from 300 to 800 nm ranged from 78.5 ± 1.8 to 97.6 ± 0.5 . The ultrastructure of gel-formed COMatrix was also characterized by scanning electron microscopy. As given in Figure 5C, known representation of collagen fibers could be seen and by increasing the concentration of COMatrix hydrogel, the fibers' density also increases.

Gelation kinetics and rheological characterization of COMatrix hydrogel

The thermoresponsive gelation kinetics of *in situ* thermoresponsive gel formation of COMatrix were characterized by recording the alterations in light absorbance of the hydrogel (turbidimetric assay) and measuring the changes in rheological indexes of COMatrix hydrogel while cured with mild heat (37°C). The turbidimetric assay showed that the COMatrix hydrogel starts to form a gel soon after exposure to mild heat. The time needed to reach 50% of maximum gelation ($t_{1/2}$) was 4 min and the gelation was completed in 10 min (Fig. 6A). The rheological gelation kinetics characterizations showed that COMatrix hydrogel had negligible gelation at 12°C (first 3 min of recording), but as soon as the temperature was increased to 37°C, gel formation started (Fig. 6B). Gel formation is indicated by the increase in both elastic (G') and viscous (G'') components of shear modulus at 37°C. Complete gel formation was achieved in 10 min. The highest elastic shear moduli (G') for 15 and 25 mg/mL hydrogels were 42.1 ± 11.4 (Pa) and 83.3 ± 4.2 (Pa), respectively, and the highest viscous moduli (G'') were 4.9 ± 2.7 (Pa) for 15 mg/mL and 12.9 ± 7.2 (Pa) for 25 mg/mL samples. Figure 6C and D shows the heat-formed COMatrix gel on the rheology machine plate and a COMatrix gel after treating with heat in a conical tube, respectively. The thermally formed gel could preserve the shape of conical tube bottom (Fig. 6D). Moreover, Supplementary Video S1 shows a gel-formed COMatrix hydrogel after rheological tests.

The rheological properties of COMatrix gel in different concentrations (15 and 25 mg/mL) was evaluated with frequency sweep and strain sweep (Fig. 6E–H). The strain sweep from 0.1% to 100% showed that the linear viscoelastic (LVE) behavior of COMatrix is $<0.631\%$ (Fig. 6E,

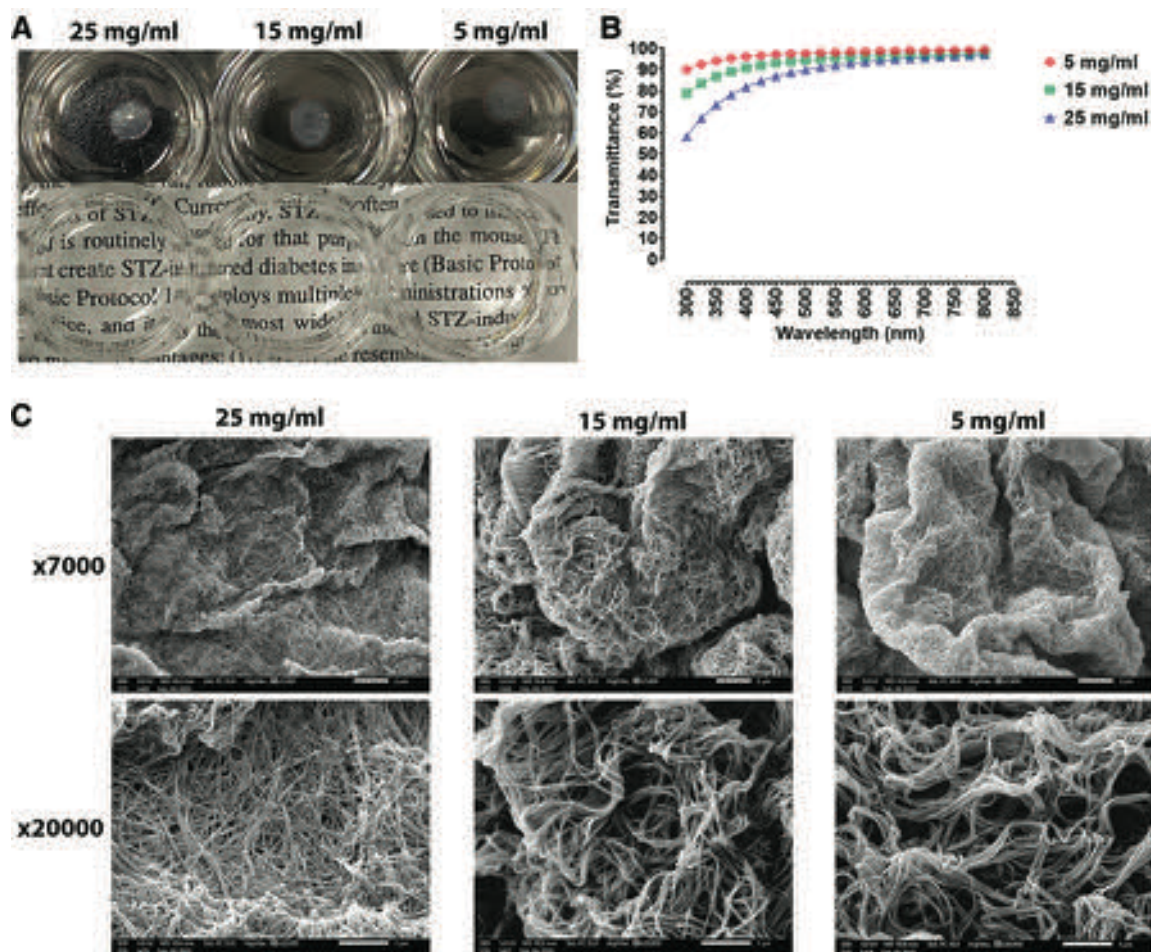


FIG. 5. Transparency and ultrastructure of COMatrix hydrogel in different concentrations. (A) Photographies showing the transparency of gel-formed COMatrix hydrogels. (B) Light transmittance of COMatrix hydrogel ($\sim 300 \mu\text{m}$ thickness) in the range of 300–800 nm. (C) The porous and fibrillar ultrastructure of COMatrix hydrogel imaged by scanning electron microscopy. Color images are available online.

G). Therefore, the 0.5% strain (in the LVE range) was used to perform the frequency sweep. The results of frequency sweep showed the gel behavior of the heat-formed COMatrix hydrogel (Fig. 6F, H).

In vitro biocompatibility of thermoresponsive COMatrix hydrogel

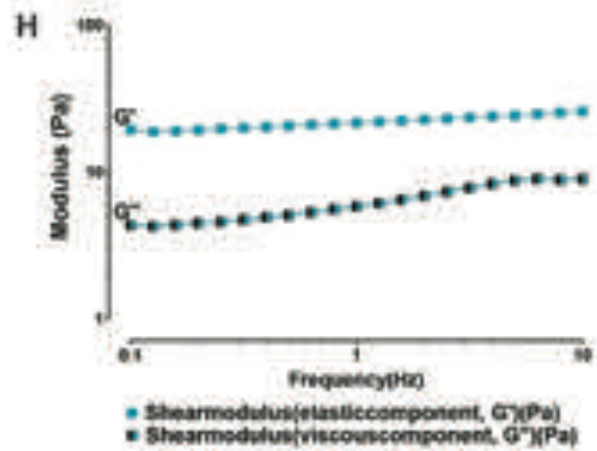
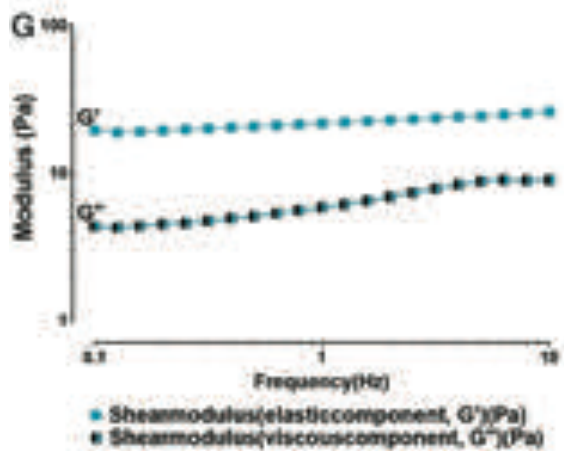
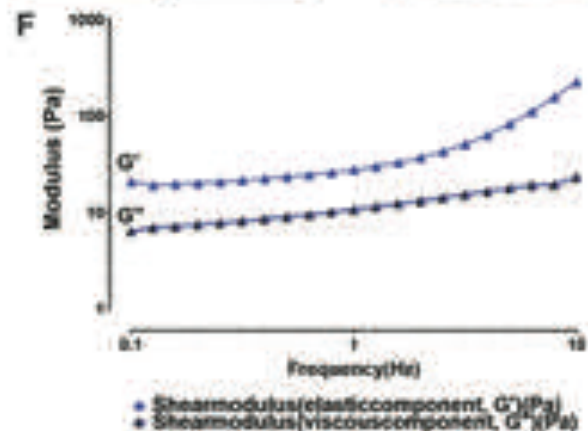
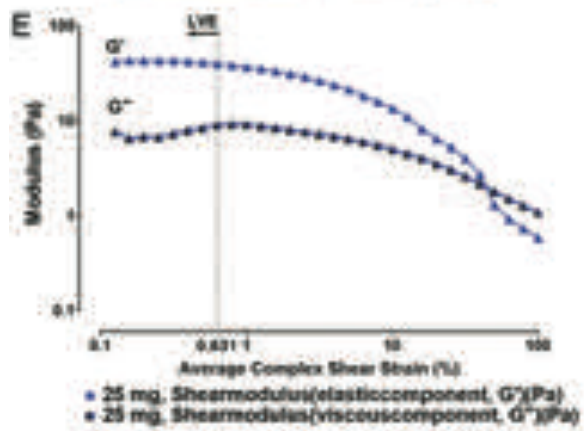
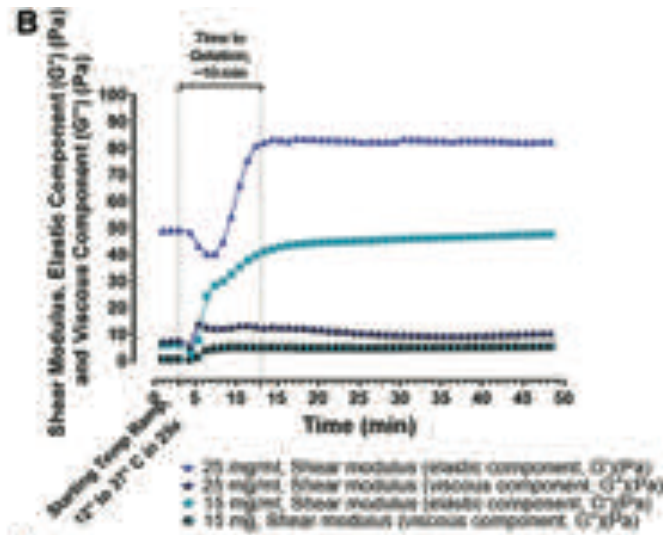
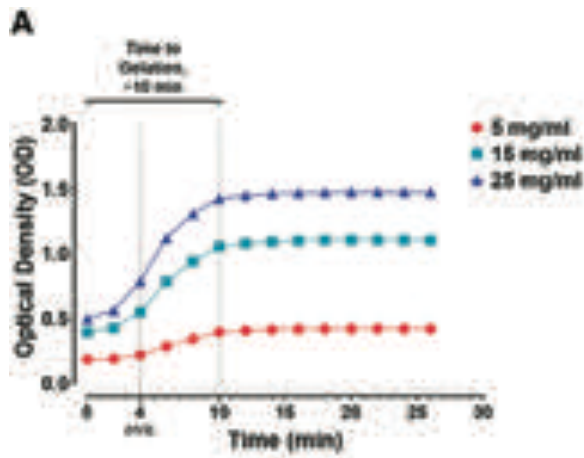
To evaluate the biocompatibility of fabricated thermoresponsive COMatrix hydrogel, HCECs were cultured on top of the gel-formed hydrogel and hMSCs were combined with COMatrix hydrogel followed by induction of gel formation by incubating at 37°C . The live-dead assay results at days 1 and 16 after culture shows significant viability of cells ($>90\%$; Fig. 7A). Moreover, the

metabolic assay representative of cells' proliferation showed that the cells are actively proliferating and the number of cells were significantly increased while cultured *in vitro* with COMatrix hydrogel (Fig. 7B).

Discussion

In this study, an *in situ* thermoresponsive and transparent hydrogel from decellularized porcine cornea ECM, COMatrix, was fabricated and characterized for further applications as an ocular therapeutic and tissue engineering biomaterial/scaffold. Structural and rheological characterization of COMatrix hydrogel showed it has the appropriate properties to be used as a scaffold for ocular tissue engineering purposes or an *in situ* hydrogel with thermal-induced sol-gel

FIG. 6. Thermal gelation kinetics of COMatrix hydrogel and rheological characterizations. (A) Turbidimetric assay results indicating the gelation of COMatrix hydrogel in ~ 10 min. (B) Gelation kinetics of COMatrix hydrogel recorded by rheological evaluation. (C) A thermally gel-formed COMatrix hydrogel on the rheometry machine bed. (D) A gel-formed COMatrix in a conical tube. The COMatrix preserves the shape of conical tube bottom. (E, F) Strain and frequency sweeps of 25 mg/mL COMatrix hydrogel. (G, H) Strain and frequency sweeps of 15 mg/mL COMatrix hydrogel. Color images are available online.



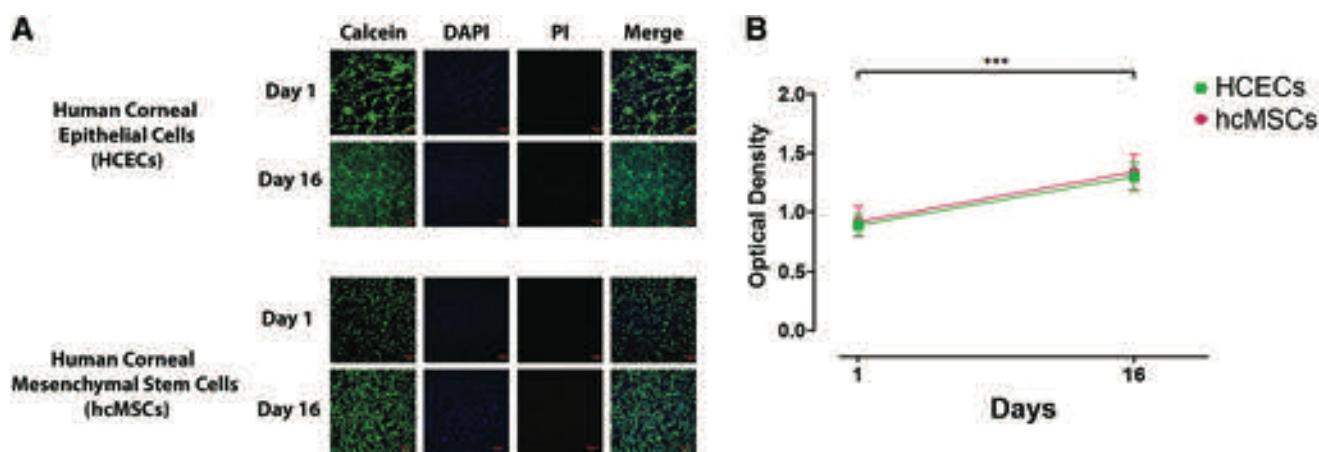


FIG. 7. Biocompatibility studies of COMatrix hydrogel. **(A)** Live-dead assay results at days 1 and 16 following culture of HCECs on top of gel-formed COMatrix hydrogel and hcMSCs combined with COMatrix hydrogel. **(B)** The result of metabolic cytotoxicity assay on the cells cultured with the thermo-gelated COMatrix showing that the fabricated hydrogel is not only toxic to the cells, but also the cells preserve the proliferation potential. $***p < 0.001$. HCEC, human corneal epithelial cell; hcMSC, human corneal mesenchymal stem cell. Color images are available online.

transition. Evaluating the protein composition of COMatrix hydrogel by mass spectrometry proteomics showed the presence of specific proteins with known corneal healing effects.

The first step in fabricating an ECM construct is to efficiently decellularize the tissue to remove all cellular components as potential antigens. There are several published decellularization protocols for cornea or amnion, which generally include applying a series of reagents followed by washing to remove cell contents.^{12,48,49} Here, we found that applying DNase is crucial for effective removal of genomic DNA. Moreover, the COMatrix hydrogel is composed of ~70% collagen and ~20% sulfated glycosaminoglycans, which is a suitable combination of these two structural molecules for tissue-scaffold engineering.

The proteomic analyses showed that >99% of the decellularized ECMs that turned into COMatrix hydrogel by partial pepsin digestion is matrixome proteins rather than intracellular proteins. This also highlights a novel application of mass spectroscopy for evaluating decellularization efficiency. Proteomic analysis revealed the presence of several proteins in COMatrix hydrogel with known corneal healing effects: lumican, laminin, and keratocan.^{31,34,42} Among these proteins detected in COMatrix, only lumican was also detected in solubilized human amnion. On the contrary, human amnion digest has proteins with known corneal healing effects like decorin and periostin.^{50,51}

In this study, the decellularized PCs were partially digested with pepsin for fabrication of a thermoresponsive hydrogel. Biologically active cryptic peptides of ECM proteins can be released by partial pepsin digestion⁵² and retained in the hydrogel and could thus contribute to the healing effects observed. It would be interesting to identify these peptic peptides by mass spectrometry and further characterize their biological properties. Of note, a limitation of this study is that it did not permit the identification of such peptides because the samples were further fully digested with trypsin before mass spectrometry analysis and only trypsin was the protease specified when conducting the database search aimed at matching peptide sequences to proteins (see Experiment

section). Future compositional proteomic studies designed to cover different digestion settings and database searches could address this concern. Moreover, because the COMatrix hydrogels were partially digested with pepsin, the downstream proteomic profiling may be biased toward the identification of pepsin-resistant proteins. However, our preliminary data do not seem to support this hypothesis, because the ECM proteins detected in decellularized corneas vastly overlapped with those forming the pepsin-digested COMatrix hydrogels (data not shown). Furthermore, given that the current report is derived from analyzing one sample of each tissue type, future in-depth MS analysis is needed to get greater coverage of the proteins already identified, but also to identify proteins present in lower abundance within the COMatrix whose detection is prevented by the hyper-abundance of collagens including other proteoglycans and ECM-associated proteins such as cytokines and growth factors.^{19,53}

Another important area worthy of investigation is the presence of cryptic peptides in decellularized ECM hydrogels. Several studies have shown the presence of functional peptide sequences inside the structure of large proteins called “cryptic peptides.”⁵⁴ The cryptic peptides are released and activated by physical or chemical alteration of large proteins such as conformational changes or proteolytic cleavages. These peptide sequences are masked in the parent protein and cannot be predicted from parent protein function or the amino acid sequence.⁵⁴ Although the effects and regulation of these peptides have yet to be understood, several studies have shown their wound healing and immunomodulatory effects.^{55,56} For instance, following an injury, inflammatory cells produce proteases that break down the macromolecule leading to the release of cryptic peptides.⁵⁷ Recent studies have indicated the skin wound healing effects of cryptic peptide sequences in structural ECM proteins like collagens,^{58,59} which could be also beneficial in corneal epithelial wound healing. To study cryptic peptides from various macromolecule sources, structural proteins such as collagens are cleaved by proteases and the cryptic peptides with biological activities are purified.⁵⁸

There are only a few studies that have performed proteomic analyses on the pepsin/HCl partially digested ECMs to explore the protein composition.⁶⁰ Williams *et al.* have shown that pepsin digestion of cardiac ECM results in exposing peptide sequences that might play a role in the cell proliferative effects of solubilized cardiac ECM.⁶⁰ The authors proposed that the highly cross-linked structure of the adult heart prevents exposition of bioactive peptides; hence, partial digestion of cardiac ECM with pepsin/HCl will uncover these peptides.⁶⁰ This could be a potential advantage of COMatrix hydrogel over intact tissues such as human amnion. The partially digested structure of COMatrix hydrogel not only provide a gel-forming regenerative biomaterial that could be easily applied on the ocular surface, but also may lead to exposure of cryptic peptides from the processed ECM that may further promote wound healing.

The results of light transmittance, structural and rheological properties of COMatrix hydrogel could be further used for ocular tissue engineering purposes. The light transmittance of human donor corneas from 450 to 600 nm is 80% to 95%,⁶¹ which is similar to the fabricated COMatrix hydrogel in this study. The exact mechanism of thermoresponsive gel formation of COMatrix hydrogel (or similar hydrogels) is not known, but it seems self-assembling feature of proteins such as collagens, laminins, and proteoglycans is playing a major role.⁶² The gelation time of COMatrix hydrogel after exposure to mild heat (37°C) is ~10 min. Moreover, the higher elastic component of shear modulus (G') compared with viscous component (G'') after completion of gelation (Fig. 6) indicates the solid-like property of gel-formed COMatrix hydrogel. The thermoresponsive feature of COMatrix has different applications in ocular regeneration. For instance, the COMatrix hydrogel could be used as an ocular surface bandage in corneal injuries; while following application of the hydrogel, the gelation could be induced with mild heat and a bandage would be formed on the ocular surface by the hydrogel.⁶³ As the gelation process of COMatrix hydrogel is more controllable compared with current materials utilized in ophthalmology, for example, fibrin glue, it has promising potential for user-friendly clinical application especially on the ocular surface. Furthermore, the COMatrix hydrogel could be used for *in situ* repair of corneal stromal defects. However, because the gel-formed COMatrix is a soft hydrogel, cross-linking protocols should be used to improve the stiffness and biomechanical stability of COMatrix for replacing the damaged corneal stroma. Depending on the performed cross-linking method, the cross-linked COMatrix might have bioadhesive properties to be attached to recipient tissue or could be fixed to the corneal stromal bed by sutures. Moreover, the utilized cross-linking method would also determine the retention time of the transplanted hydrogel until the host cells perform the remodeling process. This time needs to be longer in case of corneal stromal regeneration than other tissues, because preserving the thickness of cornea is crucial to protect the eye from perforation. This study has shown that the *in vitro* biocompatibility of COMatrix hydrogel interacted with both HCECs and hcMSCs. Future animal studies should be conducted to validate the *in vivo* applicability of COMatrix hydrogel.

Conclusion

In this study, an *in situ* thermoresponsive and transparent hydrogel, COMatrix, was fabricated and characterized from decellularized porcine cornea ECM as a potential regenerative biomaterial for ocular therapeutic and tissue engineering applications. The bioactive constituents of COMatrix that might potentially play a role in ocular regeneration include glycoproteins, proteoglycans, and cryptic peptides from collagens. In addition, the solid-like structure of COMatrix hydrogel after thermal gelation, make it a suitable candidate for *in situ* ocular repair.

Acknowledgments

The authors thank Dr. Hui Chen from the Mass Spectrometry Core facility at the University of Illinois at Chicago and the Dr. George Chlipala from the Research Informatics Core facility at the University of Illinois at Chicago for their technical assistance. This study is extracted from PhD dissertation of G.Y.

Data Availability

The raw mass spectrometry data required to reproduce these findings is available to download from the ProteomeXchange Consortium (<http://proteomecentral.proteomexchange.org>) through the PRIDE partner repository, (see methods).

Authors' Contribution

G.Y., Y.J., and B.R. carried out the experiments. G.Y. wrote the article with support from A.N. and A.D. M.O., M.R., Y.P., and T.S. helped supervise the project. A.N. and A.D. supervised the project.

Disclosure Statement

No competing financial interests exist.

Funding Information

This work was supported by R01 EY024349 (ARD), Core Grant for Vision Research EY01792 (MIR) from NEI/NIH; Unrestricted Grant to the Department and Physician-Scientist Award both from Research to Prevent Blindness; Eversight; and a Catalyst Award from the Chicago Biomedical Consortium with support from the Searle Funds at the Chicago Community Trust (grant C-088) to A.N. Proteomics services were provided by the UIC Research Resources Center Mass spectrometry Core which was established in part by a grant from The Searle Funds at the Chicago Community Trust to the Chicago Biomedical Consortium. Bioinformatic analyses were performed by the UIC Research Informatics Core, supported in part by the National Center for Advancing Translational Sciences (NCATS, Grant No. UL1TR002003).

The funders had no role in study design, data collection and analysis, decision to publish, or preparation of the article.

Supplementary Material

Supplementary Table S1
Supplementary Video S1

References

- Mathews, P.M., Lindsley, K., Aldave, A.J., and Akpek, E.K. Etiology of global corneal blindness and current practices of corneal transplantation: a focused review. *Cornea* **37**, 1198, 2018.
- Islam, M.M., Buznyk, O., Reddy, J.C., *et al.* Biomaterials-enabled cornea regeneration in patients at high risk for rejection of donor tissue transplantation. *NPJ Regen Med* **3**, 2, 2018.
- Gain, P., Jullienne, R., He, Z., *et al.* Global survey of corneal transplantation and eye banking. *JAMA Ophthalmol* **134**, 167, 2016.
- Lagali, N. Corneal stromal regeneration: current status and future therapeutic potential. *Curr Eye Res* **45**, 278, 2020.
- Hong, H., Kim, H., Han, S.J., *et al.* Compressed collagen intermixed with cornea-derived decellularized extracellular matrix providing mechanical and biochemical niches for corneal stroma analogue. *Mater Sci Eng C Mater Biol Appl* **103**, 109837, 2019.
- Matthysen, S., Van den Bogerd, B., Dhuhghaill, S.N., Koppen, C., and Zakaria, N. Corneal regeneration: a review of stromal replacements. *Acta Biomater* **69**, 31, 2018.
- Tsai, I.L., Hsu, C.C., Hung, K.H., Chang, C.W., and Cheng, Y.H. Applications of biomaterials in corneal wound healing. *J Chin Med Assoc* **78**, 212, 2015.
- Chen, Z., You, J., Liu, X., *et al.* Biomaterials for corneal bioengineering. *Biomed Mater* **13**, 032002, 2018.
- Palchesko, R.N., Carrasquilla, S.D., and Feinberg, A.W. Natural biomaterials for corneal tissue engineering, repair, and regeneration. *Adv Healthc Mater* **7**, e1701434, 2018.
- Ahearne, M., and Lynch, A.P. Early observation of extracellular matrix-derived hydrogels for corneal stroma regeneration. *Tissue Eng Part C Methods* **21**, 1059, 2015.
- Kim, H., Park, M.N., Kim, J., Jang, J., Kim, H.K., and Cho, D.W. Characterization of cornea-specific bioink: high transparency, improved in vivo safety. *J Tissue Eng* **10**, 2041731418823382, 2019.
- Shafiq, M.A., Gemeinhart, R.A., Yue, B.Y., and Djalilian, A.R. Decellularized human cornea for reconstructing the corneal epithelium and anterior stroma. *Tissue Eng Part C Methods* **18**, 340, 2012.
- Kim, H., Jang, J., Park, J., *et al.* Shear-induced alignment of collagen fibrils using 3D cell printing for corneal stroma tissue engineering. *Biofabrication* **11**, 035017, 2019.
- Wang, F., Shi, W., Li, H., *et al.* Decellularized porcine cornea-derived hydrogels for the regeneration of epithelium and stroma in focal corneal defects. *Ocul Surf* **18**, 748, 2020.
- Ahearne, M., and Fernandez-Perez, J. Fabrication of corneal extracellular matrix-derived hydrogels. *Methods Mol Biol* **2145**, 159, 2020.
- Fernandez-Perez, J., and Ahearne, M. The impact of decellularization methods on extracellular matrix derived hydrogels. *Sci Rep* **9**, 14933, 2019.
- Saldin, L.T., Cramer, M.C., Velankar, S.S., White, L.J., and Badylak, S.F. Extracellular matrix hydrogels from decellularized tissues: structure and function. *Acta Biomater* **49**, 1, 2017.
- Dziki, J.L., Wang, D.S., Pineda, C., Sicari, B.M., Rausch, T., and Badylak, S.F. Solubilized extracellular matrix bioscaffolds derived from diverse source tissues differentially influence macrophage phenotype. *J Biomed Mater Res A* **105**, 138, 2017.
- Espana, E.M., and Birk, D.E. Composition, structure and function of the corneal stroma. *Exp Eye Res* **198**, 108137, 2020.
- Deihim, T., Yazdanpanah, G., and Niknejad, H. Different light transmittance of placental and reflected regions of human amniotic membrane that could be crucial for corneal tissue engineering. *Cornea* **35**, 997, 2016.
- Cissell, D.D., Link, J.M., Hu, J.C., and Athanasiou, K.A. A modified hydroxyproline assay based on hydrochloric acid in ehrlich's solution accurately measures tissue collagen content. *Tissue Eng Part C Methods* **23**, 243, 2017.
- Naba, A., Hoersch, S., and Hynes, R.O. Towards definition of an ECM parts list: an advance on GO categories. *Matrix Biol* **31**, 371, 2012.
- Naba, A., Clauser, K.R., and Hynes, R.O. Enrichment of extracellular matrix proteins from tissues and digestion into peptides for mass spectrometry analysis. *J Vis Exp* **101**, e53057, 2015.
- Nesvizhskii, A.I., Keller, A., Kolker, E., and Aebersold, R. A statistical model for identifying proteins by tandem mass spectrometry. *Anal Chem* **75**, 4646, 2003.
- Naba, A., Clauser, K.R., Hoersch, S., Liu, H., Carr, S.A., and Hynes, R.O. The matrisome: in silico definition and in vivo characterization by proteomics of normal and tumor extracellular matrices. *Mol Cell Proteomics* **11**, M111014647, 2012.
- Naba, A., Clauser, K.R., Ding, H., Whittaker, C.A., Carr, S.A., and Hynes, R.O. The extracellular matrix: tools and insights for the "omics" era. *Matrix Biol* **49**, 10, 2016.
- Deutsch, E.W., Bandeira, N., Sharma, V., *et al.* The ProteomeXchange consortium in 2020: enabling 'big data' approaches in proteomics. *Nucleic Acids Res* **48**, D1145, 2020.
- Perez-Riverol, Y., Csordas, A., Bai, J., *et al.* The PRIDE database and related tools and resources in 2019: improving support for quantification data. *Nucleic Acids Res* **47**, D442, 2019.
- Yadavalli, T., Suryawanshi, R., Ali, M., *et al.* Prior inhibition of AKT phosphorylation by BX795 can define a safer strategy to prevent herpes simplex virus-1 infection of the eye. *Ocul Surf* **18**, 221, 2020.
- Jabbehari, S., Yazdanpanah, G., Kanu, L.N., *et al.* Reproducible Derivation and Expansion of Corneal Mesenchymal Stromal Cells for Therapeutic Applications. *Transl Vis Sci Technol* **9**, 26, 2020.
- Liu, C.Y., and Kao, W.W. Lumican promotes corneal epithelial wound healing. *Methods Mol Biol* **836**, 285, 2012.
- Coulson-Thomas, V.J., Chang, S.H., Yeh, L.K., *et al.* Loss of corneal epithelial heparan sulfate leads to corneal degeneration and impaired wound healing. *Invest Ophthalmol Vis Sci* **56**, 3004, 2015.
- Ni, M., Evans, D.J., Hawgood, S., Anders, E.M., Sack, R.A., and Fleiszig, S.M. Surfactant protein D is present in human tear fluid and the cornea and inhibits epithelial cell invasion by *Pseudomonas aeruginosa*. *Infect Immun* **73**, 2147, 2005.
- Kurpakus, M.A., Daneshvar, C., Davenport, J., and Kim, A. Human corneal epithelial cell adhesion to laminins. *Curr Eye Res* **19**, 106, 1999.
- Wang, L., Wu, X., Shi, T., and Lu, L. Epidermal growth factor (EGF)-induced corneal epithelial wound healing through nuclear factor kappaB subtype-regulated CCCTC binding factor (CTCF) activation. *J Biol Chem* **288**, 24363, 2013.

36. Jeong, W.Y., Yoo, H.Y., and Kim, C.W. Neuregulin-1 accelerates corneal epithelial wound healing. *Growth Factors* **35**, 225, 2017.
37. Brown, D.J., Lin, B., and Holguin, B. Expression of neuregulin 1, a member of the epidermal growth factor family, is expressed as multiple splice variants in the adult human cornea. *Invest Ophthalmol Vis Sci* **45**, 3021, 2004.
38. Miyagi, H., Thomasy, S.M., Russell, P., and Murphy, C.J. The role of hepatocyte growth factor in corneal wound healing. *Exp Eye Res* **166**, 49, 2018.
39. Kowtharapu, B.S., Prakasam, R.K., Murin, R., *et al.* Role of bone morphogenetic protein 7 (BMP7) in the modulation of corneal stromal and epithelial cell functions. *Int J Mol Sci* **19**, 1415, 2018.
40. Saika, S., Ikeda, K., Yamanaka, O., *et al.* Therapeutic effects of adenoviral gene transfer of bone morphogenetic protein-7 on a corneal alkali injury model in mice. *Lab Invest* **85**, 474, 2005.
41. Morishige, N., Ko, J.A., Morita, Y., and Nishida, T. Expression of semaphorin 3A in the rat corneal epithelium during wound healing. *Biochem Biophys Res Commun* **395**, 451, 2010.
42. Liu, C.Y., Chikama, T.I., Carlson, E., Perez, V.L., and Kao, W.W. Role of keratocan in corneal epithelium during wound healing. *Invest Ophthalmol Vis Sci* **46**, 2131, 2005.
43. Tan, X., Chen, Y., Foulsham, W., *et al.* The immunoregulatory role of corneal epithelium-derived thrombospondin-1 in dry eye disease. *Ocul Surf* **16**, 470, 2018.
44. Sekiyama, E., Nakamura, T., Cooper, L.J., *et al.* Unique distribution of thrombospondin-1 in human ocular surface epithelium. *Invest Ophthalmol Vis Sci* **47**, 1352, 2006.
45. Pulido, J.S., Sugaya, I., Comstock, J., and Sugaya, K. Reelin expression is upregulated following ocular tissue injury. *Graefes Arch Clin Exp Ophthalmol* **245**, 889, 2007.
46. Wolf, M., Maltseva, I., Clay, S.M., Pan, P., Gajjala, A., and Chan, M.F. Effects of MMP12 on cell motility and inflammation during corneal epithelial repair. *Exp Eye Res* **160**, 11, 2017.
47. Mulholland, B., Tuft, S.J., and Khaw, P.T. Matrix metalloproteinase distribution during early corneal wound healing. *Eye (Lond)* **19**, 584, 2005.
48. Lynch, A.P., and Ahearne, M. Strategies for developing decellularized corneal scaffolds. *Exp Eye Res* **108**, 42, 2013.
49. Gholipourmalekabadi, M., Farhadhosseinabadi, B., Faraji, M., and Nourani, M.R. How preparation and preservation procedures affect the properties of amniotic membrane? How safe are the procedures? *Burns* **46**, 1254, 2020.
50. Qu, Y.L.W., Li, C., Li, W., and Liu, Z.G. Periostin is associated with the properties of human corneal epithelial progenitor cells. *Invest Ophthalmol Vis Sci* **54**, 980, 2013.
51. Mohan, R.R., Tovey, J.C., Gupta, R., Sharma, A., and Tandon, A. Decorin biology, expression, function and therapy in the cornea. *Curr Mol Med* **11**, 110, 2011.
52. Agrawal, V., Tottey, S., Johnson, S.A., Freund, J.M., Siu, B.F., and Badylak, S.F. Recruitment of progenitor cells by an extracellular matrix cryptic peptide in a mouse model of digit amputation. *Tissue Eng Part A* **17**, 2435, 2011.
53. Taha, I.N., and Naba, A. Exploring the extracellular matrix in health and disease using proteomics. *Essays Biochem* **63**, 417, 2019.
54. Autelitano, D.J., Rajic, A., Smith, A.I., Berndt, M.C., Ilag, L.L., and Vadas, M. The cryptome: a subset of the proteome, comprising cryptic peptides with distinct bioactivities. *Drug Discov Today* **11**, 306, 2006.
55. Maquart, F.X., and Monboisse, J.C. Extracellular matrix and wound healing. *Pathol Biol (Paris)* **62**, 91, 2014.
56. Maquart, F.X., Bellon, G., Pasco, S., and Monboisse, J.C. Matrikines in the regulation of extracellular matrix degradation. *Biochimie* **87**, 353, 2005.
57. Banerjee, P., and Shanthi, C. Cryptic peptides from collagen: a critical review. *Protein Pept Lett* **23**, 664, 2016.
58. Banerjee, P., Suguna, L., and Shanthi, C. Wound healing activity of a collagen-derived cryptic peptide. *Amino Acids* **47**, 317, 2015.
59. Banerjee, P., Mehta, A., and Shanthi, C. Investigation into the cyto-protective and wound healing properties of cryptic peptides from bovine Achilles tendon collagen. *Chem Biol Interact* **211**, 1, 2014.
60. Williams, C., Sullivan, K., and Black, L.D., 3rd. Partially digested adult cardiac extracellular matrix promotes cardiomyocyte proliferation in vitro. *Adv Healthc Mater* **4**, 1545, 2015.
61. Beems, E.M., and Van Best, J.A. Light transmission of the cornea in whole human eyes. *Exp Eye Res* **50**, 393, 1990.
62. Freytes, D.O., Martin, J., Velankar, S.S., Lee, A.S., and Badylak, S.F. Preparation and rheological characterization of a gel form of the porcine urinary bladder matrix. *Biomaterials* **29**, 1630, 2008.
63. Yazdanpanah G, Shah R, Raghurama R Somala S, Anwar KN, Shen X, An S, Omid M, Rosenblatt MI, Shokuhfar T, Djalilian AR. In-situ porcine corneal matrix hydrogel as ocular surface bandage. *Ocul Surf* 2021 [Epub ahead of print]; DOI:10.1016/j.jtos.2021.04.004.

Address correspondence to:

Alexandra Naba, PhD
 Department of Physiology and Biophysics
 University of Illinois at Chicago
 909 S Wolcott Avenue, COMRB 2035
 Chicago, IL 60612
 USA

E-mail: anaba@uic.edu

Ali R. Djalilian, MD
 Department of Ophthalmology and Visual Sciences
 Illinois Eye and Ear Infirmary
 University of Illinois at Chicago
 1855 W. Taylor Street, MC 648
 Chicago, IL 60612
 USA

E-mail: adjalili@uic.edu

Received: January 20, 2021

Accepted: March 24, 2021

Online Publication Date: May 18, 2021